Journal of Dental Research
2015, Vol. 94(2) 297–303

DOI: 10.1177/0022034514559250
jdr.sagepub.com

Bioactive and Thermally Compatible Glass Coating on Zirconia Dental Implants

A. Kirsten[1], A. Hausmann[1], M. Weber[1], J. Fischer[2], and H. Fischer[1]

Abstract

The healing time of zirconia implants may be reduced by the use of bioactive glass coatings. Unfortunately, existing glasses are either bioactive like Bioglass 45S5 but thermally incompatible with the zirconia substrate, or they are thermally compatible but exhibit only a very low level of bioactivity. In this study, we hypothesized that a tailored substitution of alkaline earth metals and alkaline metals in 45S5 can lead to a glass composition that is both bioactive and thermally compatible with zirconia implants. A novel glass composition was analyzed using x-ray fluorescence spectroscopy, dilatometry, differential scanning calorimetry, and heating microscopy to investigate its chemical, physical, and thermal properties. Bioactivity was tested in vitro using simulated body fluid (SBF). Smooth and microstructured glass coatings were applied using a tailored spray technique with subsequent thermal treatment. Coating adhesion was tested on implants that were inserted in bovine ribs. The cytocompatibility of the coating was analyzed using L929 mouse fibroblasts. The coefficient of thermal expansion of the novel glass was shown to be slightly lower ($11.58 \cdot 10^{-6}$ K^{-1}) than that of the zirconia ($11.67 \cdot 10^{-6}$ K^{-1}). After storage in SBF, the glass showed reaction layers almost identical to the bioactive glass gold standard, 45S5. A process window between 800 °C and 910 °C was found to result in densely sintered and amorphous coatings. Microstructured glass coatings on zirconia implants survived a minimum insertion torque of 60 Ncm in the in vitro experiment on bovine ribs. Proliferation and cytotoxicity of the glass coatings was comparable with the controls. The novel glass composition showed a strong adhesion to the zirconia substrate and a significant bioactive behavior in the SBF in vitro experiments. Therefore, it holds great potential to significantly reduce the healing time of zirconia dental implants.

Keywords: biomaterial(s), materials science(s), ceramics, surface coated materials, endosseous dental implantation, cell culture techniques

Introduction

Dental implants made of zirconia have been increasingly in demand in recent years. The major advantage of ceramic dental implants is their tooth-like color and thereby improved aesthetics compared with titanium-based dental implants (Depprich et al. 2008). Moreover, more patients are asking for metal-free implants for biocompatibility reasons (Wenz et al. 2008). Osseointegration of zirconia is reported to be comparable with that of titanium, although clinical long-term results of this bioinert material are still lacking (Depprich et al. 2008; Gahlert et al. 2009; Koch et al. 2010). However, for both materials, a healing time of 3 to 6 months is still recommended before the definitive prosthetic restoration can be fixed (Szmukler-Moncler et al. 1998). Coatings made of bioactive glasses could reduce this time and slow down the marginal bone loss following implantation (Krajewski et al. 1996; Gomez-Vega et al. 1999; Hench 2006).

Bioglass 45S5 is still the gold standard of bioactive material (Granito et al. 2011). This glass was invented by Larry L. Hench and can create a direct chemical bond to bone within a few days in vivo (Hench 2006). However, this material is not suitable for a thermal coating process on zirconia because of its high crystallization tendency and its relatively high coefficient of thermal expansion (CTE [45S5] = $15 \cdot 10^{-6}$ K^{-1}) (Gomez-Vega et al. 1999). Zirconia exhibits a CTE of about 10.8 to $12.5 \cdot 10^{-6}$ K^{-1} (Ferraris et al. 2000; Fischer et al. 2007).

[1]Dental Materials and Biomaterials Research, RWTH Aachen University Hospital, Aachen, Germany
[2]Institute of Dental Materials and Engineering, University Hospital of Dental Medicine, University of Basel, Basel, Switzerland

A supplemental appendix to this article is published electronically only at http://jdr.sagepub.com/supplemental.

Corresponding Author:
H. Fischer, Dental Materials and Biomaterials Research, RWTH Aachen University Hospital, Pauwelsstrasse 30, 52074 Aachen, Germany.
Email: hfischer@ukaachen.de

Table. Targeted and Actual Composition (Analyzed Using XRF) of 45S5 and the Novel Glass PC-XG3.

	45S5		PC-XG3	
Oxide	Targeted Composition (wt%)	Actual Composition (wt%)	Targeted Composition (wt%)	Actual Composition (wt%)
SiO_2	45	45.53	45	44.84
CaO	24.5	24.88	22.5	21.81
MgO	—	0.06	17	17.72
Na_2O	24.5	23.18	—	0
K_2O	—	0	9.5	9.41
P_2O_5	6	6.29	6	6.15
Impurities	—	0.06	—	0.07

XRF, x-ray fluorescence spectroscopy; —, the oxide was not desired in the targeted composition (0 wt%).

Alternative glass compositions have been investigated to address these issues. Some research groups investigated bioactive glasses with a CTE near that of zirconia. Gomez-Vega et al. (1999) developed a glass composition (6P57) that exhibits a CTE of $10.8 \cdot 10^{-6}$ K^{-1}. However, because of its relatively high silica content, the bioactive behavior of this glass is very low (O'Donnell 2012). Other glasses, such as AP40 or RKKP, have also been developed as bioactive coating materials for zirconia implants (Krajewski et al. 1996). However, an invasive thermal treatment (1,300 °C) is needed to sinter these glass coatings onto the substrates, which leads to a dramatic deterioration of the zirconia microstructure at the glass-zirconia interface (Ferraris et al. 2000).

The substitution of Na_2O by K_2O and CaO by MgO (calculated in weight percent) in a silica-based glass can lead to a CTE decrease (Salmang et al. 2007; Al-Noaman et al. 2012) and a reduction of its crystallization tendency (Arstila et al. 2005; O'Donnell 2012). However, to the authors' knowledge, a glass composition with a SiO_2 content of 45 wt% and a P_2O_5 content of 6 wt% has not yet been considered to match the CTE of zirconia. In particular, the low silica content of 45 wt% could potentially retain the high bioactivity of 45S5 (Gomez-Vega et al. 1999; Hench 2006).

The hypothesis of this study is that a substitution of CaO by MgO and of Na_2O by K_2O in 45S5 Bioglass can lead to a glass composition that is both thermally compatible with zirconia and highly bioactive. Therefore, we investigated a new glass composition and analyzed its relevant properties in vitro. If the novel glass coating exhibits a high bioactivity and good adhesive strength, it holds a high potential to reduce the healing time of zirconia implants in vivo.

Materials and Methods

Preparation and Analysis

The glass composition of Bioglass 45S5 was modified by a partial substitution of Na_2O and CaO by K_2O and MgO, until a CTE below $10 \cdot 10^{-6}$ K^{-1} was calculated (see Appendix for details). A glass composition that accomplished this requirement was synthesized (Table; see Appendix for details).

Glass specimens with dimensions of 5 × 5 × 20 mm were prepared (see Appendix for details) for dilatometry measurements, which were performed with 5 K/min from room temperature up to the dilatometric softening point T_d (Dil402E; Netzsch, Selb, Germany). Zirconia was analyzed using cylindrical specimens with a diameter of 5 mm and a height of 20 mm. Two specimens per material were measured. The CTE was calculated from 100 °C up to a temperature of 50 °C below the transition temperature (T_g – 50 °C).

The sintering behavior of the fine glass powder was analyzed by means of a heating microscope with automatic image processing (EM-201; Hesse Instruments, Osterode, Germany) to identify a suitable process window. A glass suspension was prepared (see Appendix for details) and applied onto polished zirconia specimens using a spray nozzle (model 97; Düsen-Schlick, Untersiemau, Germany) to produce homogeneous coatings. Smooth glass coatings (Gs) were produced by spraying the glass suspension onto substrates and firing the specimens at 830 °C for 100 min (Austromat 3001; DEKEMA, Freilassing, Germany). X-ray diffraction (XRD, D8 Advance; Bruker AXS, Karlsruhe, Germany) was used to investigate the crystallization behavior of the sintered glass coatings. Microstructured glass coatings (Gm) were produced by spraying a second layer of glass suspension onto a densely sintered first coating and conducting a subsequent sintering process at 760 °C for 10 min. The coatings had a thickness of around 20 to 50 µm after sintering. Cross sections were prepared (see Appendix for details) and investigated using scanning electron microscopy (SEM, FEI ESEM XL30 FEG; Philips, Eindhoven, the Netherlands).

In Vitro Bioactivity

In vitro bioactivity tests were performed using simulated body fluid (SBF). Cylindrical bulk glass specimens with a diameter of 15 mm and a thickness of 1 mm were polished with diamond suspensions to 1 µm. The specimens were stored in the SBF solution for 1, 3.5, 7, 14, and 28 d. A detailed protocol of this test is described elsewhere (Kokubo and Takadama 2006; International Organization for Standardization [ISO] 2014). 45S5 Bioglass samples were

manufactured as described by Plewinski et al. (2013) and used as reference samples. The surface reaction layers were investigated using SEM and energy dispersive x-ray spectroscopy (EDS, Falcon Genesis; EDAX, Mahwah, NJ, USA) and x-ray diffractometry (XRD, D8 Advance; Bruker AXS, Karlsruhe, Germany).

Insertion Tests

Insertion tests of zirconia dental implants (type ceramic. implant; VITA Zahnfabrik, Bad Säckingen, Germany) were performed to estimate the adhesion of the glass coatings, mimicking the clinical situation. Hence, bovine ribs of a 6- to 8-y-old heifer were used. Implant beds were prepared according to the instructions of the implant manufacturer (VITA Zahnfabrik) with a guided drilling machine (PBD 40; Bosch, Stuttgart, Germany) to ensure a defined cavity. Threads were cut inside the bone prior to implant insertion. Zirconia implants exhibited a lathed surface without any roughening before coating. Six implants were coated following the above-described process to create microstructured glass coatings (Gm) with a thickness of 20 to 30 µm. Five implants were inserted using a torque wrench (Holex 200; Hoffmann Qualitätswerkzeuge, Munich, Germany) by applying an insertion torque of 60 Ncm. Subsequently, the implants were unscrewed, washed carefully with gauze in distilled water, and dried with compressed air. The bones were then sawn along the implant axis to investigate the thickness of the cortical bone. One implant with a microstructured glass coating was not inserted and served as control. The implant surfaces were investigated using SEM.

Cytocompatibility

Cell culture experiments were performed using L929 mouse fibroblasts (Gibco, Paisley, Scotland). Proliferation and cytotoxicity assays were applied. The following specimens were tested: Zp, polished zirconia; Zm, microstructured zirconia (ceramic.implant; VITA Zahnfabrik); Gs, smooth glass surface on polished zirconia; and Gm, microstructured glass surface on polished zirconia. Cell culture glass (P231.1; Carl Roth, Karlsruhe, Germany) was used as reference. Proliferation was analyzed with a cell viability assay (CellTiter-Blue Cell Viability Assay; Promega, Madison, WI, USA) after 1, 2, 3, and 4 d to investigate cell growth on the different surfaces, which can provide additional information about their cytocompatibility. Cytotoxicity was analyzed using Cytotox-ONE Assay (Promega) on days 1 and 4 (see Appendix for details).

Laser scanning microscopy (LSM) was performed at 200-fold magnification (VK-X110; Keyence, Osaka, Japan) (n = 6) to evaluate the surface roughness parameters of identically prepared samples. Statistical analyses for LSM, proliferation, and cytotoxicity tests were performed using 1-way analysis of variance (ANOVA) with the Tukey post hoc test (α = 0.05; SPSS version 20; SPSS, Inc., an IBM Company, Chicago, IL, USA).

Results

The maximum deviation between target and actual values of the oxides of the 2 synthesized glasses was only 0.7 wt% for PC-XG3 and 0.8 wt% for 45S5 (Table). The novel glass PC-XG3 had a slightly lower thermal expansion coefficient (below its glass transition temperature, T_g) than the ceramic substrate (Fig. 1A). CTEs were $11.67 \cdot 10^{-6}$ K^{-1} (100–640 °C) for 3Y-TZP, $11.58 \cdot 10^{-6}$ K^{-1} for PC-XG3 (100–640 °C), and $16.92 \cdot 10^{-6}$ K^{-1} for 45S5 (100–470 °C). Glass transition temperatures (T_g) were 692 °C for PC-XG3 and 519 °C for 45S5. Dilatometric softening points (T_d) were 730.5 °C for PC-XG3 and 560.5 °C for 45S5. Differential scanning calorimetry (DSC) measurement of glass PC-XG3 confirmed the value for T_g and showed a peak crystallization temperature of 989 °C. Crystallization of this glass started at about 910 °C (T_C). The silhouette of a cylinder made of the glass powder changed with increasing temperature (Fig. 1B). The height and area of this silhouette began to decrease after reaching T_g and revealed the softening point (T_S) at around 800 °C. The T_C from DSC measurements is shown in Figure 1B to illustrate the process window of this glass.

Both glasses, 45S5 and PC-XG3, exhibited a Si-rich layer of about 20 µm and a CaP-rich layer of about 10 µm after 14 days of storage in SBF (Fig. 2A, B). Carbonated hydroxyapatite was found after 3.5 to 7 d on both glasses (Fig. 2C, D).

XRD results proved that no crystallization occurred after sintering of the glass coatings (Fig. 3A). The peaks detected belong to the Y-TZP substrate (tetragonal zirconia). No additional peaks occurred. Figure 3B shows a cross section of the densely sintered smooth glass coating (Gs). Figure 3C shows a cross section including the second glass layer, which was not densely sintered and thereby created a microstructure on the surface (Gm).

The glass coating was not affected by the insertion and subsequent unscrewing of the implant (Fig. 3D–3I). In fact, bone particles remained on the unaffected microstructured glass surface (Fig. 3I). Unscrew torques of up to 140 Ncm were measured. The thickness of cortical bone was 2 to 5 mm.

Laser scanning microscopy revealed the following roughness values (according to ISO 1997): control: Ra = 0.049 ± 0.005, Rz = 8.26 ± 1.78; Zp: Ra = 0.048 ± 0.004, Rz = 6.91 ± 3.00; Zm: Ra = 1.756 ± 0.05, Rz = 31.12 ± 4.61; Gs: Ra = 0.322 ± 0.075, Rz = 17.81 ± 5.18; Gm: Ra = 5.379 ± 0.7, Rz = 93.78 ± 7.18 (means and standard deviations are reported, all values in µm). Statistically significant differences were found between all pairs except control and Zp using the Tukey post hoc test (n = 6, α = 0.05). The proliferation rate of L929 mouse fibroblasts on the novel glass coating was comparable during the first 4 d (Fig. 4A). Novel

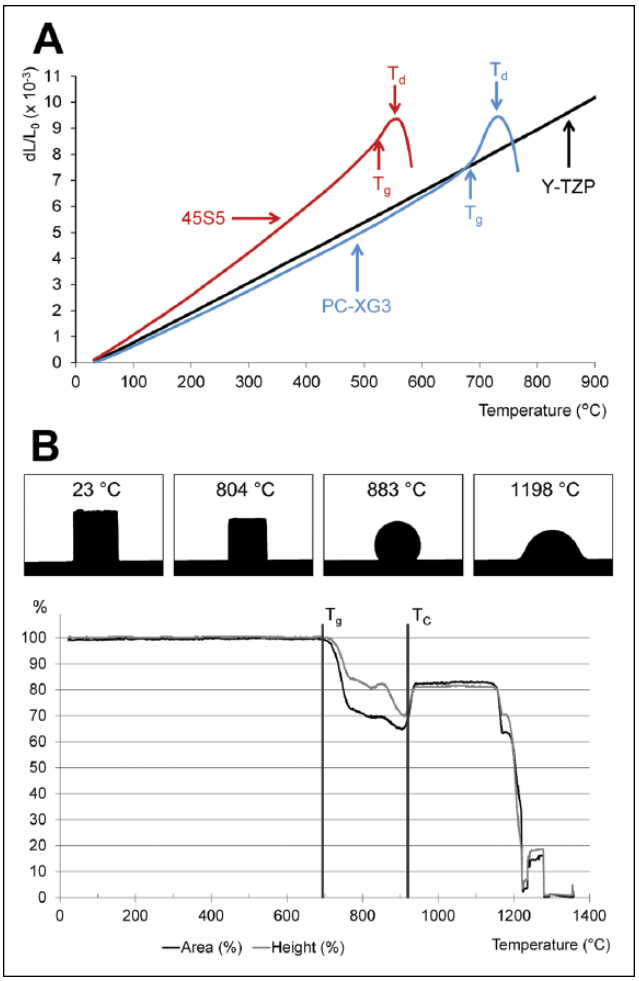

Figure 1. Thermal characterization. (**A**) Thermal expansion behavior of Y-TZP, 45S5, and PC-XG3. T_g, glass transition temperature; T_d, dilatometric softening point. (**B**) Results of heating microscope measurements for PC-XG3. Exemplary silhouettes and relative silhouette changes (of area and height) dependent on temperature are shown. T_g and T_C are added from differential scanning calorimetry measurements.

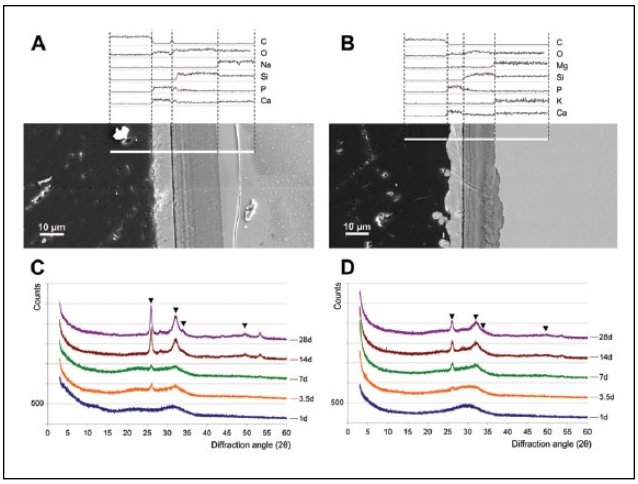

Figure 2. 45S5 (**A**, **C**) and PC-XG3 (**B**, **D**) after storage in simulated body fluid (SBF). A and B show exemplary cross sections of the resulting surface layers after 14 d. Bulk glass is shown on the right side and the embedding material on the left side of the picture. White lines represent the zones of elemental analysis. C and D show x-ray diffraction results after 1 to 28 days of storage. Each diagram was scaled up about 500 counts for easier reading. The marked peaks correspond with carbonate hydroxyapatite (powder diffraction file 00-019-0272, database PDF4+ [2009]; International Centre for Diffraction Data, Newtown Square, PA, USA).

glass coatings did not cause statistically significant differences in cell proliferation. In all cases, the cytotoxicity was very low (~10%) and at the level of the control (Fig. 4B).

Discussion

The CTE of the novel glass composition PC-XG3 was adapted to the CTE of Y-TZP (Fig. 1A), giving the basic requirement for good coating stability. Compared with 45S5, the CTE of PC-XG3 was mainly decreased because of the substantial replacement (in wt%) of CaO and Na_2O by MgO and K_2O. This can be attributed to the thermal expansion factors in semi-empirical glass models such as the Appen factors. A lower Appen factor leads to a decrease in thermal expansion. For instance, the Appen factor of MgO (6) is much lower than that of CaO (13) or Na_2O (39.5) (Salmang et al. 2007). The Appen factor of K_2O (42) is higher compared with that of Na_2O (Salmang et al. 2007). However, the atomic weight of this oxide is greater than Na_2O. Therefore, calculating in weight percent, K_2O also exhibits a lowering effect on the CTE when it replaces Na_2O. However, the CTE of the glass was higher than calculated by the SciGlass software (SciMatic, Newton, MA, USA), which calculated a CTE of $9.5 \cdot 10^{-6}\ K^{-1}$ for this composition. This discrepancy can be explained by the fact that the glass composition described here could not be interpolated using glasses in the database (Priven 2004). The software uses an extrapolation routine, which is always accompanied by a certain inaccuracy. The CTE of Y-TZP was in the range of reported values for this material ($10.8–12.5 \cdot 10^{-6}\ K^{-1}$) (Ferraris et al. 2000; Fischer et al. 2007). The CTE of PC-XG3 was about $0.09 \cdot 10^{-6}\ K^{-1}$ lower than the CTE of the substrate material (below its T_g). The CTE of a coating material should be slightly below the CTE of the substrate (Fischer et al. 2007). This strategy leads to desirable compressive stresses in the glass coating and thereby improves the mechanical reliability of a quasi-brittle coating (Evans et al. 1983). This strategy is also used on veneering materials for all-ceramic partial dentures (Fischer et al. 2007).

Bioglass 45S5 remains the gold standard for a synthetic material with a pronounced bioactive behavior (Hench 2006; Granito et al. 2011). Therefore, 45S5 was selected as reference material for the in vitro bioactivity tests using SBF. The PC-XG3 glass showed a behavior in SBF comparable with

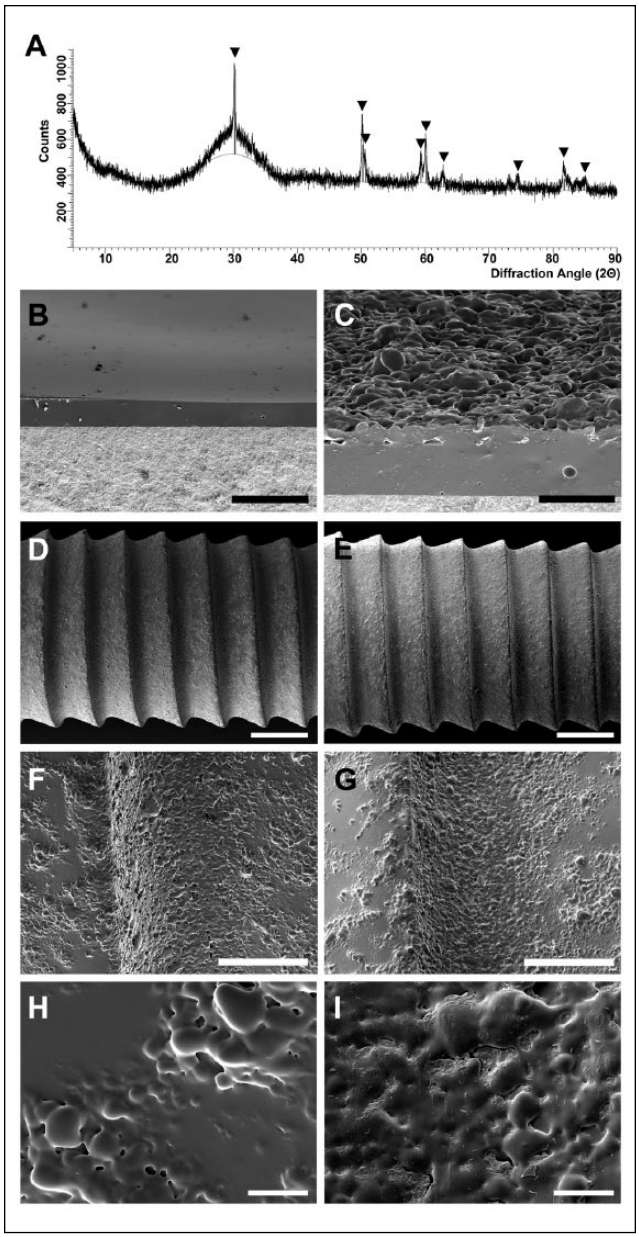

Figure 3. Glass coatings made of PC-XG3 on Y-TZP substrate. (**A**) X-ray diffraction measurement of sintered glass coating after heat treatment at 830 °C for 100 min. The marked peaks correspond with tetragonal zirconia (powder diffraction file 01-083-0113, database PDF4+ [2009]; International Centre for Diffraction Data, Newtown Square, PA). (**B**) Cross section of a densely sintered glass coating after heat treatment at 830 °C for 100 min (smooth glass coating [Gs]). (**C**) Cross section of a microstructured glass coating (Gm) achieved by sintering a second glass layer onto the first sintered layer at 760 °C for 10 min. (**D–I**) Scanning electron micrographs of implants with microstructured glass coatings (Gm) before (D, F, H) and after (E, G, I) implant insertion into bovine ribs. Scale bars: B and C, 50 µm; D and E, 1 mm; F and G, 200 µm; H and I, 20 µm.

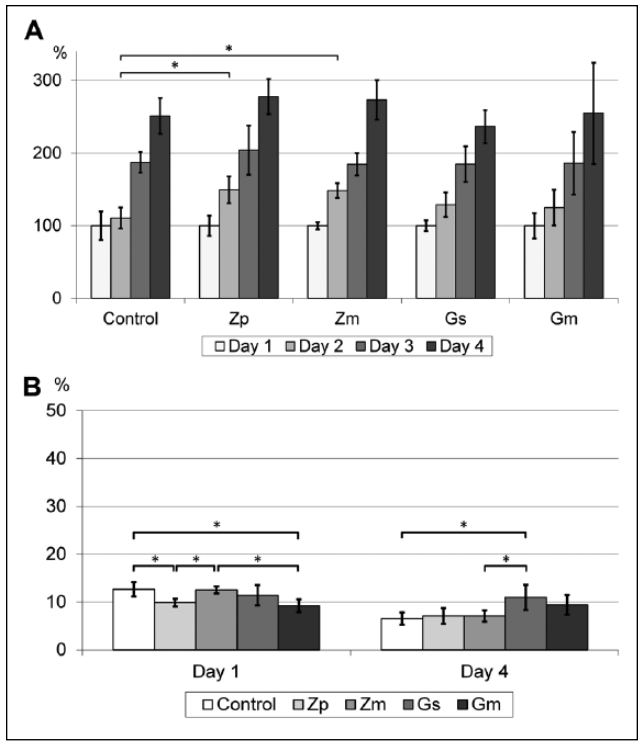

Figure 4. Normalized proliferation (**A**) and cytotoxicity (**B**) of L929 mouse fibroblasts. Control, cell culture glass; Zp, polished Y-TZP; Zm, microstructured Y-TZP; Gs, smooth glass coatings (PC-XG3); Gm, microstructured glass coatings (PC-XG3). Means and standard deviations are shown (n = 6). *Significant difference, analyzed using the Tukey post hoc test (P < 0.05).

45S5. The mechanism of bioactive glasses in SBF is described elsewhere (Kokubo and Takadama 2006). The silica-rich and Ca/P-rich layers showed comparable thickness and morphology after the same storage time for both glasses (Fig. 2A, B). The crystallinity of the Ca/P-rich layer was also similar (Fig. 2C, D). Carbonated hydroxyapatite was found as the main crystalline phase, and the first peaks were detected after 3.5 to 7 d for both PX-XG3 and 45S5. Bloyer et al. (2007) showed that bioactive glasses with potassium and magnesium can exhibit the same mechanism in SBF as 45S5. However, other glasses developed as coating materials did not show as high a level of bioactivity in direct comparison with 45S5 (Gomez-Vega et al. 1999; Ferraris et al. 2000; Lopez-Esteban et al. 2003; Al-Noaman et al. 2012). Thus, the new glass shows a high potential to reduce the healing time of dental implants when used as coating material. Bohner and Lemaitre (2009) and Pan et al. (2010) doubted that in vivo bioactivity could be predicted after storage of a material in SBF. Therefore, the promising results of PC-XG3 should not be overemphasized. A definitive estimation of its bioactivity can only be made after in vivo experiments, which are already planned for the novel glass composition.

The process window for PC-XG3 was determined by DSC and heating microscopy (Fig. 1B). Sintering of the glass occurred at approximately 800 °C (T_S), and crystallization began at approximately 910 °C (T_C). A thermal

treatment at 830 °C for 100 min led to a densely sintered coating without any crystallization (Fig. 3A, B). No cracks or delamination were found. This proves that the thermal expansion coefficients of coating and substrate were well adjusted. The surface of most current implants exhibits a microstructure to improve osseointegration (Buser et al. 1991; Zechner et al. 2003; Abrahamsson et al. 2004). Therefore, a microstructured glass surface was created with a second layer of the novel glass that was sintered using a tailored thermal treatment. Good bonding between the first and the second glass layers was confirmed (Fig. 3C).

Implant insertion tests were performed to estimate the bonding quality between the substrate and glass coating. Bovine ribs were used for this purpose because they exhibit comparable mechanical properties with human alveolar bone (Bredbenner and Haug 2000). The thickness of cortical bone has a significant influence on the implant insertion torque (Elias et al. 2012). Therefore, a minimal thickness of 1.5 mm was ensured in this study, which corresponds to the corticalis of human alveolar bone (Katranji et al. 2007). In fact, the cortical thickness of the bones used here was 2 to 5 mm. According to the manufacturer's instructions, these dental implants must be inserted with a torque of 25 to 35 Ncm (surgical.guide 2014; VITA Zahnfabrik). However, in this study, a minimal torque of 60 Ncm was applied to induce a much higher stress on the glass coating. In addition, the implants were unscrewed after the insertion. During this explantation, a much higher torque (up to 140 Ncm) was necessary to remove the implants because of static friction. Despite the fairly extreme stress that was applied to the glass coatings during these tests, SEM evaluation did not reveal any cracks or delamination after explantation of the implants (Fig. 3E, G, I). Thus, a very high adhesion of the glass coatings to the zirconia implants was proven. It is of particular interest that the implant surfaces were only lathed but not roughened before coating. This could be a great advantage for future applications of ceramic implants because a roughened or microstructured surface of a quasi-brittle component always leads to a decrease in strength (Salmang et al. 2007). As a positive side effect, the microstructured glass coating presented here could help to improve the mechanical reliability of a ceramic dental implant.

L929 mouse fibroblasts were seeded onto the specimens to evaluate cytocompatibility with a well-established cell line (Suzuki et al. 1999). All specimens were found to be cytocompatible. The proliferation test showed significant differences only between the control and the zirconia specimens (Zp, Zm) for day 2. We found statistically significant differences concerning the cytotoxicity tests between the groups for day 1 and day 4. However, those differences varied for day 1 and day 4. Therefore, cytotoxicity on smooth and microstructured glass coatings (Gs and Gm) was comparable with the references and far below the threshold value of 30%, which is required by the ISO standard (Fig. 4) (ISO 2009). Roughness values of the specimens differed significantly. The microstructured novel glass coatings (Gm) exhibited a much higher surface roughness than all other groups, including Zm. However, proliferation and cytotoxicity of the mouse fibroblasts were not influenced by surface topology. In a comparative study, Kunzler et al. (2007) investigated the influence of surface roughness on the proliferation of human osteoblasts and fibroblasts. A higher surface roughness led to a strong increase in proliferation of osteoblasts. However, the influence of surface roughness on the proliferation of fibroblasts was much lower in their study. They even reported a slightly decreasing fibroblast cell growth with a higher surface roughness. The good cytocompatibility results in this study revealed that the basic requirements are fulfilled with respect to a clinical usage of the novel glass coatings.

The novel glass coating developed in this study exhibits a high potential to accelerate healing after insertion of zirconia dental implants in a subsequent in vivo application. This estimation is only given based on tests in SBF and therefore has limited validity. However, as those results are very motivating, we will investigate this novel bioactive glass coating's in vivo behavior to investigate its bone bonding and degradation behavior in a subsequent study.

Author Contributions

A. Kirsten, contributed to conception, design, data acquisition, analysis, and interpretation, drafted the manuscript; A. Hausmann, contributed to data analysis and interpretation, critically revised the manuscript; M. Weber, contributed to data acquisition and analysis, critically revised the manuscript; J. Fischer, contributed to conception, design, and data interpretation, critically revised the manuscript; H. Fischer, contributed to conception, design, data analysis, and interpretation, critically revised the manuscript. All authors gave final approval and agree to be accountable for all aspects of the work.

Acknowledgments

The authors thank Wolfgang Wilsmann and Tanja Mund from the Department of Glass and Ceramic Composites, Institute of Mineral Engineering, RWTH Aachen for their help concerning the thermal analysis of the novel glass. They also thank Peter König, Margit Kehren, and Petra Schott from the Department of Ceramics and Refractory Materials, Institute of Mineral Engineering, RWTH Aachen for their help concerning laser granulometry, x-ray fluorescence spectroscopy, and x-ray diffraction analysis. Stefan Rütten from the Electron Microscopy Facility, RWTH Aachen University Hospital is thanked for his help concerning SEM and EDS analysis. Dr. Hendrik Meyer Lückel and Dr. Marcella Esteves Oliveira from the Department of Operative Dentistry, Periodontology and Preventive Dentistry are thanked for their help concerning laser scanning microscopy. The authors are grateful to VITA Zahnfabrik, Bad Säckingen, Germany, for financial support and for providing zirconia dental implants for the experiments. The authors declare no potential conflicts of interest with respect to the authorship and/or publication of this article.

References

Abrahamsson I, Berglundh T, Linder E, Lang NP, Lindhe J. 2004. Early bone formation adjacent to rough and turned endosseous implant surfaces: an experimental study in the dog. Clin Oral Implants Res. 15(4):381–392.

Al-Noaman A, Rawlinson SCF, Hill RG. 2012. The role of MgO on thermal properties, structure and bioactivity of bioactive glass coating for dental implants. J Non Cryst Solids. 358(22):3019–3027.

Arstila H, Zhang D, Vedel E, Hupa L, Ylänen HO, Hupa M. 2005. Bioactive glass compositions suitable for repeated heat-treatments. Key Eng Mater. 284–286:925–928.

Bloyer DR, McNaney JM, Cannon RM, Saiz E, Tomsia AP, Ritchie RO. 2007. Stress-corrosion crack growth of Si-Na-K-Mg-Ca-P-O bioactive glasses in simulated human physiological environment. Biomaterials. 28(33):4901–4911.

Bohner M, Lemaitre J. 2009. Can bioactivity be tested in vitro with SBF solution? Biomaterials. 30(12):2175–2179.

Bredbenner TL, Haug RH. 2000. Substitutes for human cadaveric bone in maxillofacial rigid fixation research. Oral Surg Oral Med Oral Pathol Oral Radiol Endod. 90(5):574–580.

Buser D, Schenk RK, Steinemann S, Fiorellini JP, Fox CH, Stich H. 1991. Influence of surface characteristics on bone integration of titanium implants: a histomorphometric study in miniature pigs. J Biomed Mater Res. 25(7):889–902.

Depprich R, Zipprich H, Ommerborn M, Naujoks C, Wiesmann HP, Kiattavorncharoen S, Lauer HC, Meyer U, Kübler NR, Handschel J. 2008. Osseointegration of zirconia implants compared with titanium: an in vivo study. Head Face Med. 4:30.

Elias CN, Rocha FA, Nascimento AL, Coelho PG. 2012. Influence of implant shape, surface morphology, surgical technique and bone quality on the primary stability of dental implants. J Mech Behav Biomed Mater. 16:169–180.

Evans AG, Crumley GB, Demaray RE. 1983. On the mechanical behavior of brittle coatings and layers. Oxid Met. 20(5–6):193–216.

Ferraris M, Verné E, Appendino P, Moisescu C, Krajewski A, Ravaglioli A, Piancastelli A. 2000. Coatings on zirconia for medical applications. Biomaterials. 21(8):765–773.

Fischer J, Stawarczyk B, Tomic M, Strub JR, Hämmerle CH. 2007. Effect of thermal misfit between different veneering ceramics and zirconia frameworks on in vitro fracture load of single crowns. Dent Mater J. 26(6):766–772.

Gahlert M, Röhling S, Wieland M, Sprecher CM, Kniha H, Milz S. 2009. Osseointegration of zirconia and titanium dental implants: a histological and histomorphometrical study in the maxilla of pigs. Clin Oral Implants Res. 20(11):1247–1253.

Gomez-Vega JM, Saiz E, Tomsia AP. 1999. Glass-based coatings for titanium implant alloys. J Biomed Mater Res. 46(4):549–559.

Granito RN, Rennó AC, Ravagnani C, Bossini PS, Mochiuti D, Jorgetti V, Driusso P, Peitl O, Zanotto ED, Parizotto NA, et al. 2011. In vivo biological performance of a novel highly bioactive glass-ceramic (Biosilicate®): a biomechanical and histomorphometric study in rat tibial defects. J Biomed Mater Res B Appl Biomater. 97(1):139–147.

Hench LL. 2006. The story of Bioglass®. J Mater Sci Mater Med. 17(11):967–978.

International Organization for Standardization (ISO). 1997. Geometrical Product Specifications (GPS)—surface texture: profile method—terms, definitions and surface texture parameters. Geneva, Switzerland: ISO. ISO document 4287:1997.

International Organization for Standardization (ISO). 2009. Biological evaluation of medical devices—part 5: tests for in vitro cytotoxicity. Geneva, Switzerland: ISO. ISO Document 10993:2009–5.

International Organization for Standardization (ISO). 2014. Implants for surgery—in vitro evaluation for apatite-forming ability of implant materials. Geneva, Switzerland: ISO. ISO document 23317:2014.

Katranji A, Misch K, Wang HL. 2007. Cortical bone thickness in dentate and edentulous human cadavers. J Periodontol. 78(5):874–878.

Koch FP, Weng D, Krämer S, Biesterfeld S, Jahn-Eimermacher A, Wagner W. 2010. Osseointegration of one-piece zirconia implants compared with a titanium implant of identical design: a histomorphometric study in the dog. Clin Oral Implants Res. 21(3):350–356.

Kokubo T, Takadama H. 2006. How useful is SBF in predicting in vivo bone bioactivity? Biomaterials. 27(15):2907–2915.

Krajewski A, Malavolti R, Piancastelli A. 1996. Albumin adhesion on some biological and non-biological glasses and connection with their Z-potentials. Biomaterials. 17(1):53–60.

Kunzler TP, Drobek T, Schuler M, Spencer ND. 2007. Systematic study of osteoblast and fibroblast response to roughness by means of surface-morphology gradients. Biomaterials. 28(13):2175–2182.

Lopez-Esteban S, Saiz E, Fujino S, Oku T, Suganuma K, Tomsia AP. 2003. Bioactive glass coatings for orthopedic metallic implants. J Eur Ceram Soc. 23(15):2921–2930.

O'Donnell MD. 2012. Melt-derived bioactive glass. In: Jones JR, Clare AG, editors. Bio-glasses. Chichester (UK): Wiley. p. 13–28.

Pan H, Zhao X, Darvell BW, Lu WW. 2010. Apatite-formation ability—predictor of "bioactivity"? Acta Biomater. 6(11):4181–4188.

Plewinski M, Schickle K, Lindner M, Kirsten A, Weber M, Fischer H. 2013. The effect of crystallization of bioactive bioglass 45S5 on apatite formation and degradation. Dent Mater. 29(12):1256–1264.

Priven AI. 2004. General method for calculating the properties of oxide glasses and glass-forming melts from their composition and temperature. Glass Technol. 45(6):244–254.

Salmang H, Scholze H, Telle R, editors. 2007. Keramik. Heidelberg (Germany): Springer.

Suzuki T, Ohashi R, Yokogawa Y, Nishizawa K, Nagata F, Kawamoto Y, Kameyama T, Toriyama M. 1999. Initial anchoring and proliferation of fibroblast L-929 cells on unstable surface of calcium phosphate ceramics. J Biosci Bioeng. 87(3):320–327.

Szmukler-Moncler S, Salama H, Reingewirtz Y, Dubruille JH. 1998. Timing of loading and effect of micromotion on bone-dental implant interface: review of experimental literature. J Biomed Mater Res. 43(2):192–203.

Wenz HJ, Bartsch J, Wolfart S, Kern M. 2008. Osseointegration and clinical success of zirconia dental implants: a systematic review. Int J Prosthodont. 21(1):27–36.

Zechner W, Tangl S, Furst G, Tepper G, Thams U, Mailath G, Watzek G. 2003. Osseous healing characteristics of three different implant types: a histologic and histomorphometric study in mini-pigs. Clin Oral Implants Res. 14(2):150–157.